Acta Crystallographica Section D
Biological Crystallography
ISSN 0907-4449

Caged and clustered structures of endothelin inhibitor BQ123, cyclo(-D-Trp-D-Asp$^-$-Pro-D-Val-Leu-)·Na$^+$, forming five and six coordination bonds between sodium ions and peptides

Mitsunobu Doi,[a]* Akiko Asano,[a] Toshimasa Ishida,[a] Yoshio Katsuya,[b] Yoshihiro Mezaki,[b] Masahiro Sasaki,[c] Akira Terashima,[c] Taizo Taniguchi,[c] Hiroshi Hasegawa[c] and Masaaki Shiono[d]

[a]Osaka University of Pharmaceutical Sciences, 4-20-1 Nasahara, Takatsuki, Osaka 569-1094, Japan, [b]Hyogo Prefectural Institute of Industrial Research, 3-1-12 Yukihira-cho, Suma, Kobe 654-0037, Japan, [c]Hyogo Institute for Aging Brain and Cognitive Disorders, 520 Saisho-ko, Himeji 670-0981, Japan, and [d]Kyushu University, Hakozaki, Higashi-ku, Fukuoka-shi 812-8581, Japan

Correspondence e-mail: doit@oysun01.oups.ac.jp

Received 26 September 2000
Accepted 9 February 2001

BQ123 is a cyclic pentapeptide and a potent endothelin-1 inhibitor. The crystal structure of the BQ123 sodium salt was determined as the first example of an endothelin inhibitor. Four independent molecules and many solvent molecules were found in the asymmetric unit; the total weight was about 3000 Da. The precise structure including the solvent molecules was determined using high-resolution data collected on a synchrotron source. Sodium ions formed unique structures with five and six coordination bonds and their forms were distinguished into three classes. An ion was sandwiched by two BQ123 molecules. This peptide–sodium (2:1) complex showed a cage-like structure and octahedral coordination was observed. Sodium ions also formed a cluster composed of hydrated water molecules and peptides. Two sodium ions were contained in this cluster, making five coordination bonds. Despite having the same coordination numbers, these ions were distinguishable by differences in the polyhedra. One was trigonal bipyramidal (having six planes) and the other was square pyramidal (having five planes). Both shapes were very similar to each other, although the synchrotron data clearly revealed slight geometrical differences.

1. Introduction

Endothelin (ET) is an endogenous vasoconstriction peptide with 21 amino-acid residues (Yanagisawa *et al.*, 1988). Since its activity is linked to the regulation of blood pressure, this peptide has been targeted to develop antagonists for therapeutic applications for hypertension (Gulati, 1995). Two cyclic peptapeptides, BE18257A [cyclo(D-Trp-D-Glu-Ala-D-Val-Leu)] and BE18257B [cyclo(D-Trp-D-Glu-Ala-*allo*-D-Ile-Leu)], were isolated from *Streptomyces misakiensis* (Kojiri *et al.*, 1991; Nakajima *et al.*, 1991; Ihara *et al.*, 1991) which antagonized the ET-1 induced vasoconstriction by binding to the endothelin A (ET_A) receptor subtype (IC_{50} values are 1.40 and 0.47 μM for BE18257A and BE18257B, respectively; Ishikawa *et al.*, 1992). The more potent ET-1 antagonist BQ123 [cyclo(D-Trp-D-Asp-Pro-D-Val-Leu)] has subsequently been surveyed (IC_{50} = 7.3 nM; Ihara *et al.*, 1992; Fukami *et al.*, 1995). In addition to the screening of ET antagonists, structural studies have also been performed (Hewage *et al.*, 1997); the helical property was observed in the C-terminal region (Okada *et al.*, 1991; Van der Walle *et al.*, 1998). Such a structural feature was also confirmed in the crystal structure of ET-1 (Peapus *et al.*, 1993; Janes *et al.*, 1994). A recent NMR study suggested that the structures of these antagonists were partially similar to that of ET-1 (Coles *et al.*, 1993; Peishoff *et al.*, 1995). These structural studies for both intrinsic substrates

Table 1
Coordination bond lengths and angles and hydrogen bonds found in the caged structures.

(*a*) Na1.

Atom1	Atom1—Na1 distance (Å)	Atom1—Na1—Atom2 angle (°) Atom2 D-Asp22 O	D-Asp12 O	D-Asp12 OD1	D-Asp22 OD1	D-Val24 O
D-Asp22 O	2.263 (3)					
D-Asp12 O	2.280 (4)	168.8 (1)				
D-Asp12 OD1	2.375 (4)	101.2 (1)	81.8 (1)			
D-Asp22 OD1	2.375 (4)	79.8 (1)	111.3 (1)	87.8 (1)		
D-Val24 O	2.459 (4)	81.7 (1)	87.1 (1)	99.9 (1)	161.0 (1)	
D-Val14 O	2.471 (4)	95.2 (1)	81.9 (1)	163.6 (1)	96.2 (1)	81.3 (1)

Hydrogen bonds.

D	*A*	*D*···*A* (Å)	H···*A* (Å)	*D*—H···*A* (°)
D-Trp11 N	D-Asp22 OD1	2.776 (5)	1.962	157.4
D-Asp12 N	D-Asp12 OD1	2.779 (5)	2.271	117.9
D-Val14 N	D-Val24 O	3.020 (5)	2.377	132.0
D-Trp21 N	D-Asp12 OD2	2.812 (6)	1.965	167.9
D-Val24 N	D-Val14 O	2.999 (5)	2.356	131.9

(*b*) Na2.

Atom1	Atom1—Na2 distance (Å)	Atom1—Na2—Atom2 angle (°) Atom2 D-Asp32 O	D-Asp42 O	D-Asp42 OD1	D-Asp32 OD1	D-Val44 O
D-Asp32 O	2.247 (4)					
D-Asp42 O	2.288 (3)	175.5 (2)				
D-Asp42 OD1	2.338 (4)	101.2 (1)	80.3 (1)			
D-Asp32 OD1	2.387 (5)	79.4 (1)	105.1 (1)	81.4 (1)		
D-Val44 O	2.502 (4)	91.9 (1)	86.6 (1)	166.9 (1)	101.1 (2)	
D-Val34 O	2.519 (4)	82.7 (1)	92.9 (1)	101.9 (2)	162.0 (1)	79.7 (1)

Hydrogen bonds.

D	*A*	*D*···*A* (Å)	H···*A* (Å)	*D*—H···*A* (°)
D-Trp31 N	D-Asp42 OD2	2.764 (6)	1.916	168.1
D-Asp32 N	D-Asp32 OD1	3.066 (5)	2.630	112.7
D-Val34 N	D-Val44 O	3.084 (5)	2.546	121.6
D-Trp41 N	D-Asp32 OD1	2.996 (5)	2.340	133.2
D-Asp42 N	D-Asp42 OD1	2.929 (5)	2.450	115.7
D-Val44 N	D-Val34 O	3.054 (5)	2.455	127.3

Table 2
Coordination bond lengths and angles and hydrogen bonds found in the cluster structure.

Na3.

Atom1	Atom1—Na3 distance (Å)	Atom1—Na3—Atom2 angle (°) Atom2 D-Trp11 O^{i}	Wat51 O1	Wat54 O1	Wat52 O1
D-Trp11 O^{i}	2.277 (4)				
Wat51 O1	2.292 (4)	109.4 (1)			
Wat54 O1	2.330 (4)	88.7 (2)	88.7 (2)		
Wat52 O1	2.340 (4)	147.2 (2)	102.2 (1)	100.9 (1)	
Leu15 O^{i}	2.384 (4)	87.5 (1)	91.3 (1)	175.9 (1)	83.1 (1)

Na4.

Atom1	Atom1—Na4 distance (Å)	Atom1—Na4—Atom2 angle (°) Atom2 Wat55 O1	Pro33 O^{ii}	Leu35 O^{ii}	Wat53 O1	Wat51 O1
Wat55 O1	2.243 (4)					
Pro33 O^{ii}	2.354 (3)	119.6 (2)				
Leu35 O^{ii}	2.373 (4)	85.5 (2)	103.5 (1)			
Wat53 O1	2.376 (4)	154.2 (2)	85.6 (1)	82.8 (1)		
Wat51 O1	2.383 (4)	81.5 (2)	83.5 (1)	167.0 (1)	109.0 (1)	
Wat54 O1	2.847 (4)	80.7 (2)	148.5 (1)	101.9 (1)	79.4 (1)	75.7 (1)

Hydrogen bonds.

D	*A*	*D*···*A* (Å)	H···*A* (Å)	*D*—H···*A* (°)
Wat51 O1	Wat55 O1	3.022 (5)	2.052	177.7
Wat51 O1	Pro13 O^{i}	2.709 (5)	1.758	179.0
Wat52 O1	Pro23 O	2.696 (5)	1.731	178.0
Wat52 O1	Leu25 O	2.797 (5)	1.792	178.0
Wat53 O1	Leu45 O	2.698 (6)	1.645	162.2
Wat53 O1	D-Trp41 O	2.888 (5)	1.857	165.8
Wat54 O1	Pro43 O	2.885 (5)	1.883	177.6
Wat54 O1	D-Trp41 O	3.011 (5)	2.015	176.5
Wat55 O1	Wat52 O1	2.797 (6)	1.758	178.8
Wat55 O1	D-Trp31 O^{ii}	2.788 (5)	1.797	178.9
Wat56 O1	D-Trp21 O	2.786 (5)	1.831	179.0
Wat56 O1	Wat51 O1	2.803 (5)	1.840	176.1
Wat57 O1	Pro43 O	2.869 (5)	1.909	177.7
Wat57 O1	Leu35 O^{ii}	2.891 (4)	1.896	178.1
Wat58 O1	Leu15 O^{i}	2.979 (5)	1.925	177.6

Symmetry codes: (i) $-x+\frac{1}{2}, -y+2, z+\frac{1}{2}$; (ii) $x+\frac{1}{2}, -y+\frac{3}{2}, -z+1$.

and antagonists are important in the characterization of the structure specificity of the ET_A receptor. We have previously reported the preliminary structure of the BQ123 sodium salt (Doi *et al.*, 2000). A more detailed discussion of the structure is now presented here.

2. Experimental

10 mg of BQ123 (M_r = 610.7, 16.4 µmol; Bachem Co.) was dissolved in 0.8 ml of 60% isopropanol (20.5 m*M*) in a 3 ml vial and 33 µl of 0.5 *M* NaOH was added (the ratio of the peptide to sodium ion was 1.0). This vial was sealed with 3.0–3.5 ml of 100% isopropanol (iPr) at room temperature and clusters of plate-shaped crystals were obtained after one week.

A total of 12 056 reflection intensity measurements, of which 6702 reflections were $\geq 3\sigma$, were collected on a Rigaku AFC5R four-circle diffractometer to 1.0 Å resolution. After exhaustive trials, the structure of the peptide was finally solved utilizing the electron-density-modification method incorporated in the program *LODEM* (Matsugaki & Shiono, 1998). In the *LODEM* procedure, a density map calculated from normalized structure factors (an *E* map) is modified repeatedly by the function

$$\begin{cases} \rho'(\mathbf{r}) = \rho(\mathbf{r})\left(1 - \exp\{-(1/2)[\rho(\mathbf{r})/0.2\rho_c]^2\}\right) & \rho(\mathbf{r}) \geq 0 \\ \rho'(\mathbf{r}) = 0 & \rho(\mathbf{r}) < 0 \end{cases},$$

where $\rho(\mathbf{r})$ and $\rho'(\mathbf{r})$ are the prior and modified electron density at $\mathbf{r}$, respectively. This removes negative density as well as sharpening peaks. ρ_c is the expected average peak height in the *E* map. A total of 6702 $|E|$s greater than unity were phased

and used for the E-map calculation. A multi-solution strategy was employed and 100 trials were performed starting from completely random phase sets. As a figure of merit, the linear correlation coefficients between $|E|$s and normalized Fourier coefficients of the modified map, $|E'|$s, of unused reflections were used, defined by

$$\mathrm{LCFOM} = \frac{\langle(|E| - \langle|E|\rangle)(|E'| - \langle|E'|\rangle)\rangle}{[\langle(|E| - \langle|E|\rangle)^2\rangle\langle(|E'| - \langle|E'|\rangle)^2\rangle)]^{1/2}},$$

where averages are taken over all reflections which are not used for the density modification. A set out of 100 trials indicated a very high LCFOM value of 0.51 and we obtained the peptide structure by surveying the resultant map.

However, the structural refinement failed because of the poor intensity data set distribution. To improve the data quality, measurements were reattempted on SPring-8/BL24XU-A (utilizing the 'figure-8' undulator and a double-crystal monochromator system; Matsui *et al.*, 1997). For data collection, optimal cryo-conditions were sought. Flash-freezing of crystals with the mother solution (aqueous isopropanol) resulted in the growth of ice or phase separation. Instead, crystals were soaked in 100% glycerol for 10–30 s and then frozen in a nitrogen-gas stream at 100 K. In this case, the crystal was partially dissolved in the glycerol, becoming smaller but leading to a better result. A total of 82 images, each with an oscillation angle of 2.2°, were collected at a wavelength of 0.836 Å and processed using *MOSFLM* (Leslie, 1990) and the *CCP*4 suite (Collaborative Computational Project, Number 4, 1994). Two data sets were prepared: one with the reflection set as orthorhombic and the other set as $P1$. Since the refinement only converged at a relatively high value of R_1 (~0.15) for the orthorhombic data, the data processed as $P1$ were adopted and then merged in *SHELXL*97 (Sheldrick, 1997). Crystal data: space group, $P2_12_12_1$; Z = 4; unit-cell parameters, a = 25.3930 (4), b = 34.7193 (3), c = 25.7201 (4) Å; V = 22675.5 (5) Å^3; $F(000)$ = 6461; μ = 0.071 mm^{-1}; a total of 83 268 reflections were merged to 22 865 unique reflections;

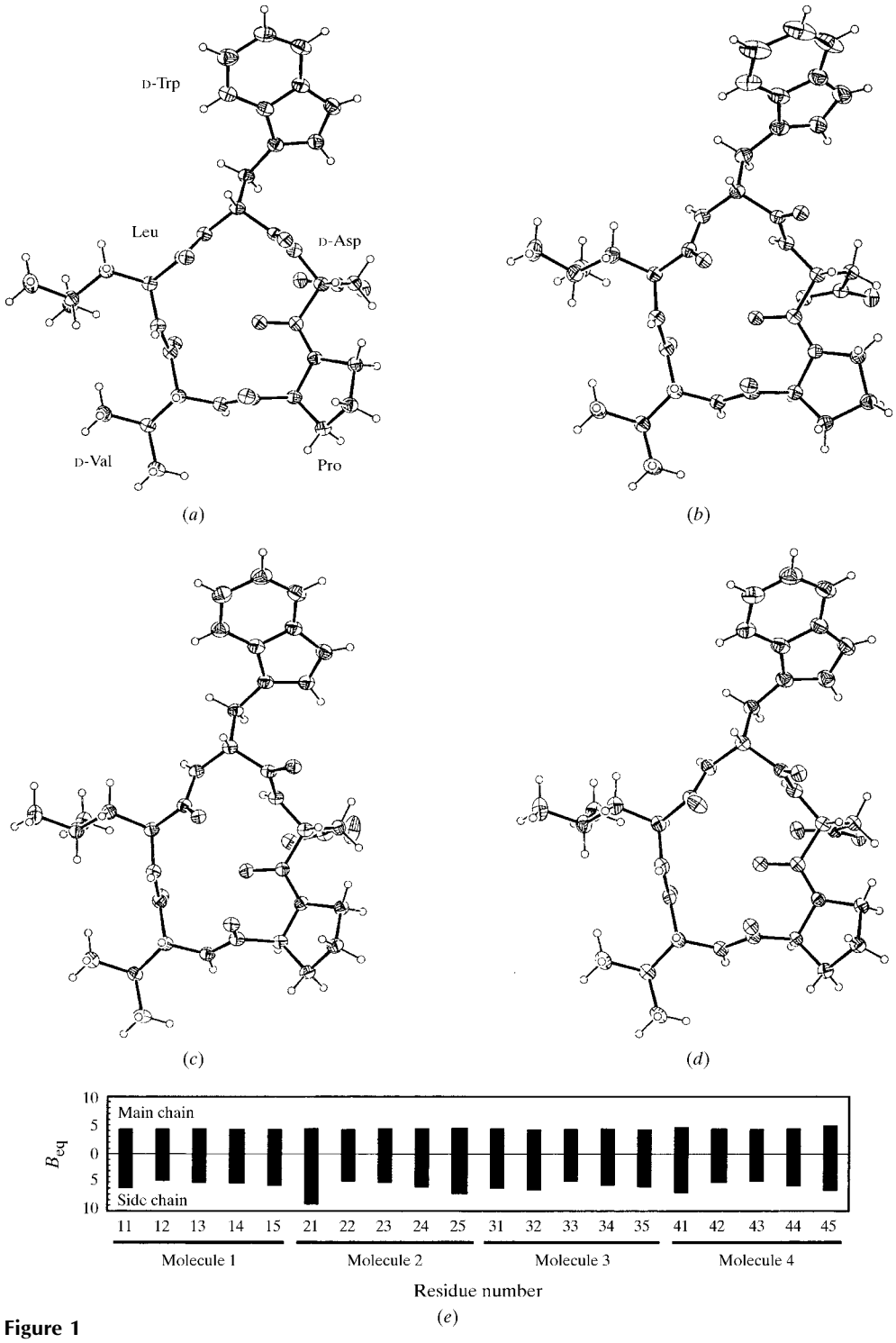

Figure 1
ORTEP (Burnett & Johnson, 1996) drawings of independent molecules and averaged temperature factors. (*a*), (*b*), (*c*) and (*d*) show molecules 1, 2, 3 and 4, respectively. (*e*) Temperature factors of the backbone and side chain are averaged for each residue. The values of B_{eq} are calculated from U_{ij}.

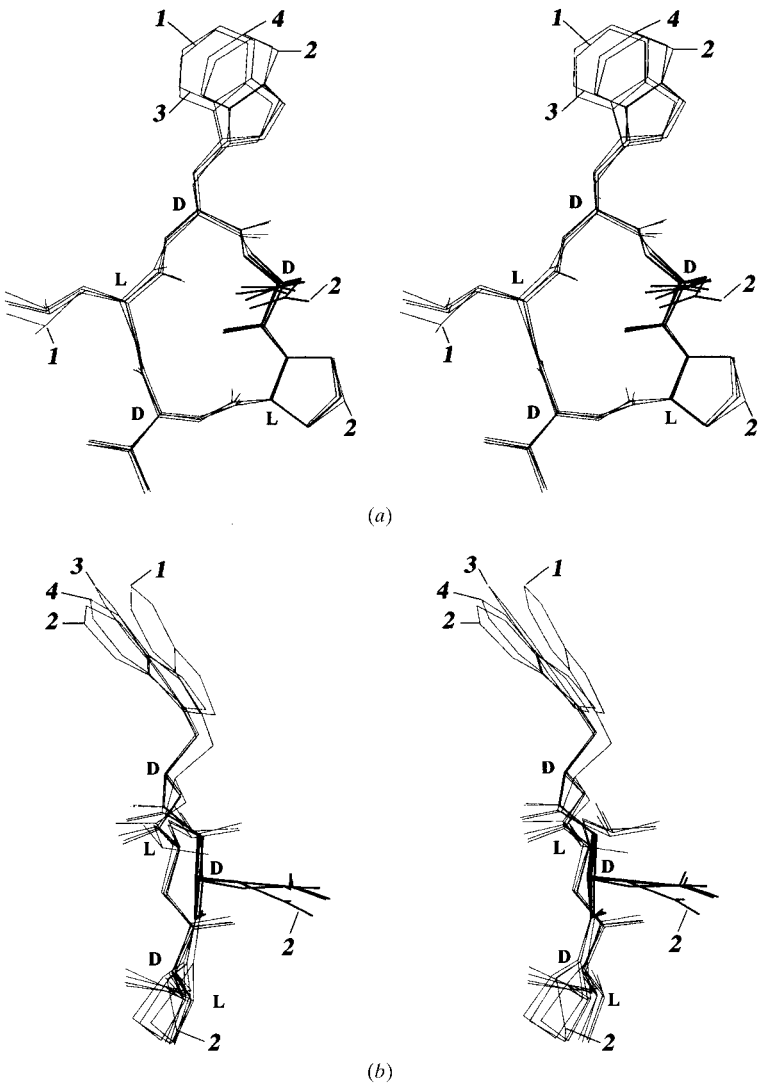

Figure 2
Superimposition of independent molecules. Projection on (*a*) the 15-membered ring and (*b*) its orthogonal view. Italic numbers represent the number of molecules. The characters D and L show the chirality of the relevant C^{α} atom. Thick lines represent D-Asp residues. This figure was produced using *SWISS-PDBVIEWER* (Guex & Peitsch, 1997).

$\theta_{>\max}$ = 31.5° (0.80 Å resolution); $R_{\rm int}$ = 0.0342. There were four BQ123 molecules in the asymmetric unit, where molecules 1, 2, 3 and 4 have amino-acid residue numbers 11–15, 21–25, 31–35 and 41–45, respectively. The chirality of the amino acids agreed with the reported sequences (Fukami *et al.*, 1995) and the calculated Flack *x* parameter was 0 (10). By computing a difference Fourier, eight water molecules (residue numbers 51–58) and six iPr sites (residue numbers 61–66) were found and included in the model refinement. The peptide H atoms were calculated at the geometrically ideal positions by the 'ride-on' method and the H atoms of solvent molecules were picked from a Fourier map considering hydrogen-bonding networks. Finally, the formula for the asymmetric unit was $4(C_{31}H_{41}N_6O_7Na)\cdot8(H_2O)\cdot5.63(C_3H_7OH)$ and M_r = 3013.12. The refinement, for 1904 parameters, converged at R_1 = 0.0576 and wR = 0.1642.

3. Molecular structure

Four independent peptide molecules occur in the asymmetric unit, each with a similar conformation (Fig. 1). To compare the structures, molecules 2, 3 and 4 were superimposed on molecule 1 using the C^{α} atoms (Fig. 2), for which the r.m.s. deviations were 0.0495, 0.0598 and 0.04814 Å, respectively. Conformational differences are seen for the bulky side chains (D-Trp and Leu), which have the largest thermal motions (Fig. 1*e*); the largest temperature factor is observed on the Trp side chain of molecule 2 (the averaged $B_{\rm eq}$ is 8.8 $Å^2$). The different puckering of the Pro residue is also observed in molecule 2 (Fig. 2). In contrast, the conformations of the backbones agree. In particular, the dispositions of the polar atoms (>N—H and ═O) are conserved. The planes of the amide bonds are arranged perpendicular to the relatively flat 15-membered rings, except for that of D-Asp. Furthermore, the disposition of the D-Asp side chain is different from those of D-Trp, D-Val and Leu (Fig. 2*b*). Although the conformations are affected by coordination to the sodium ion (discussed later), the chiral sequence of BQ123 (-D-D-L-D-L-) seems to be important for these structures. The disposition of side chains is roughly 'equatorial–axial–equatorial–equatorial–equatorial' for the sequence D-Trp-D-Asp-Pro-D-Val-Leu. It is proposed, on seeing the molecular conformation, that any chiral modifications would lead to a significant structural change. Indeed, the chemical modification of the chirality affected the inhibitory activity (Nakajima *et al.*, 1991).

4. Caged structures between peptides and ion

The sodium ion is sandwiched between two peptide molecules having octahedral (bipyramidal) coordination; two different complexes are formed with similar coordinate bonds in the crystal (Fig. 3). The bond distances between the sodium ion and carbonyl O atoms of the peptide are in the range 2.2–2.5 Å (Table 1)[1] and the order of magnitude of the coordination distance is D-Asp O—Na < D-Asp OD1—Na < D-Val O—Na in each complex. The angles D-Asp OD1—Na—O D-Val are constricted to between 160 and 170° and the octahedral coordination of the sodium ions is slightly distorted. Each D-Asp residue in the complexes provides the ligand atoms D-Asp O (backbone carbonyl group) and D-Asp OD1 (side-chain carboxyl group); this residue seems to be very important for the formation of the sodium complex. Hydrogen bonds are also observed between two peptide molecules of the complex (Table 1). The complex finally shows a 'sodium-caged' structure constructed by interactions among the D-amino acids.

[1] Supplementary data for this paper are available from the IUCr electronic archive (Reference: he0271). Services for accessing these data are described at the back of the journal.

Table 3
Hydrogen bonds formed in the linkages Na—D-Asp···D-Trp and Na—D-Asp···iPr···D-Trp.

D	*A*	*D*···*A* (Å)	H···*A* (Å)	*D*—H···*A* (°)
Wat58 O1	iPr61 O1^{i}	2.825 (6)	1.786	178.6
iPr61 O1	D-Asp22 OD2	2.760 (5)	1.810	179.3
iPr62 O1	D-Asp12 OD2	2.685 (7)	1.774	175.2
iPr63 O1	D-Asp42 OD2	2.657 (8)	1.649	177.8
iPr64 O1	D-Asp32 OD2	2.633 (9)	1.707	177.7
iPr65 O1	iPr62 O1^{i}	3.154 (19)	2.187	176.8
iPr66 O1	D-Asp32 OD2	3.025 (14)	2.107	178.7
D-Trp11 NE1	iPr63 O1^{ii}	2.776 (9)	1.918	174.8
D-Trp21 NE1	iPr64 O1^{iii}	2.802 (11)	1.945	175.4
D-Trp31 NE1	D-Asp22 OD2^{iv}	2.822 (7)	2.109	140.0
D-Trp41 NE1	iPr62 O1^{i}	2.873 (8)	2.033	165.8
Leu15 N	Wat56 O1^{ii}	2.940 (5)	2.135	155.8
Leu35 N	Wat53 O1^{iv}	2.976 (5)	2.126	170.2

Symmetry codes: (i) $\frac{1}{2}-x, 2-y, z+\frac{1}{2}$; (ii) $\frac{1}{2}-x, 2-y, z-\frac{1}{2}$; (iii) $x+\frac{1}{2}, \frac{3}{2}-y, 1-z$; (iv) $x-\frac{1}{2}$, (iv) $x-\frac{1}{2}, \frac{3}{2}-y, 1-z$.

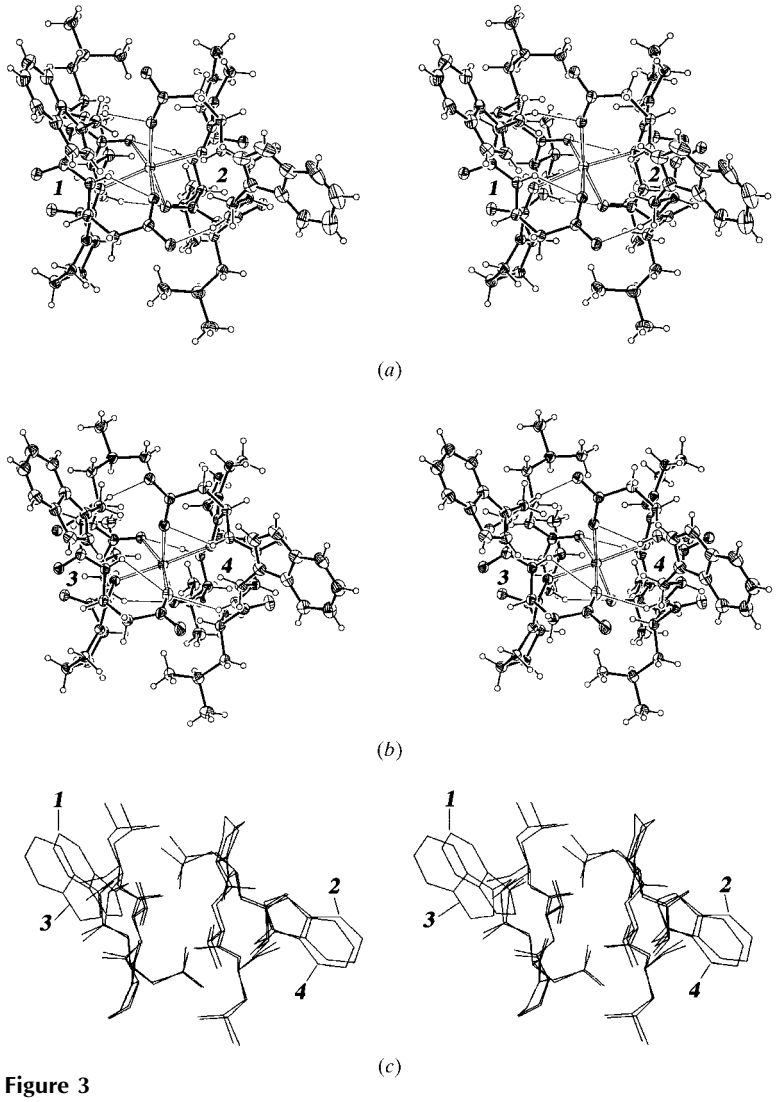

Figure 3
Stereoview of caged structures. Open bonds and thin lines represent coordination bonds and hydrogen bonds, respectively. The complexes include (*a*) Na1 and (*b*) Na2 atoms. (*c*) Superimposition of two complexes, in which H atoms are omitted for clarity. Italic numbers represent the independent molecules.

To compare the peptide structures of the two complexes, the molecular fit was calculated using the C^{α} atoms (r.m.s. deviation of 0.0601 Å) and is shown in Fig. 3(*c*). In the caged structures, the conformation of peptide backbones is conserved in four molecules. However, the Trp side chains significantly disperse in a manner which is different from that of the superimposition of each molecule (Fig. 1); this seems to be the result of hydrogen bonds between the indole ring and solvent molecules and the higher thermal motions of the Trp side chains.

5. Cluster structure formed among sodium ions, peptides and solvent molecules

The other coordination modes of the sodium ions are shown in Fig. 4 and the related geometrical parameters are listed in Table 2. Two sodium ions (Na3 and Na4) are coordinated to the peptide and water molecules and create a cluster. The Na3 atom coordinates to five O atoms (D-Trp11 O, Leu15 O, Wat51 O1, Wat52 O1 and Wat54 O1). The bond angle Leu15 O—Na3—O Wat54 is 175.9 (1)°. Three other coordinated atoms (D-Trp11 O, Wat51 O1 and Wat52 O1) create a plane perpendicular to this axis. This Na3 complex is trigonal bipyramidal and is different from the octahedral (bipyramidal) complexes of the Na1 and Na2 atoms. On the other hand, Na4 shows a coordination form similar to an octahedron. Although this ion has five coordination bonds to Pro33 O, Leu35 O, Wat51 O1, Wat53 O1 and Wat55 O1, the bond length Na4···O1 Wat54 [2.847 (4) Å] is clearly longer than the others (Verbist *et al.*, 1971). Therefore, this 'linkage' seems to be an ionic or electrostatic interaction rather than a coordination bond. The Na4 atom has five ligands, making a square plane perpendicular to the Na4—O Pro33 axis and shows a square-pyramidal form which is different to that of the Na3 complex (trigonal bipyramidal).

In this cluster structure, the water molecules which are not coordinated to the ion (Wat56, Wat57 and Wat58) are hydrogen-bonded to the coordinated O atoms, stabilizing the structure. The crystal includes the solvent molecules iPr and water, although water molecules are only found close to the sodium ions.

6. Interactions between Trp side chains and solvent molecules

The indole rings of the D-Trp residues interact with 2-propanol molecules (iPr) and the side chains of D-Asp residues as shown in Fig. 5. The geometries of the hydrogen bonds are listed in Table 3. D-Trp31 NE1 of molecule 3 is hydrogen bonded to D-Asp22 OD2 of molecule 2 and D-Asp12 OD2 is linked to iPr62 O1, which is also the acceptor in hydrogen bonds with D-Trp41 NE1 and iPr65 O1

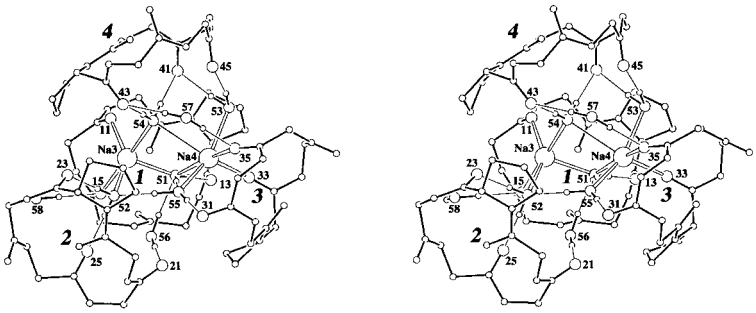

Figure 4
Stereoview of cluster structure. Side chains and H atoms of peptides are omitted for clarity and H atoms of solvents are drawn. Open bonds and thin lines represent coordination bonds and hydrogen bonds, respectively. The line between Na4 and Wat54 O1 shows the ionic or electrostatic interaction. O atoms related to coordination and hydrogen bonds are represented by larger circles and the sodium ions are represented by the biggest circles. Italic numbers represent the independent molecules; other numbers represent the residue number.

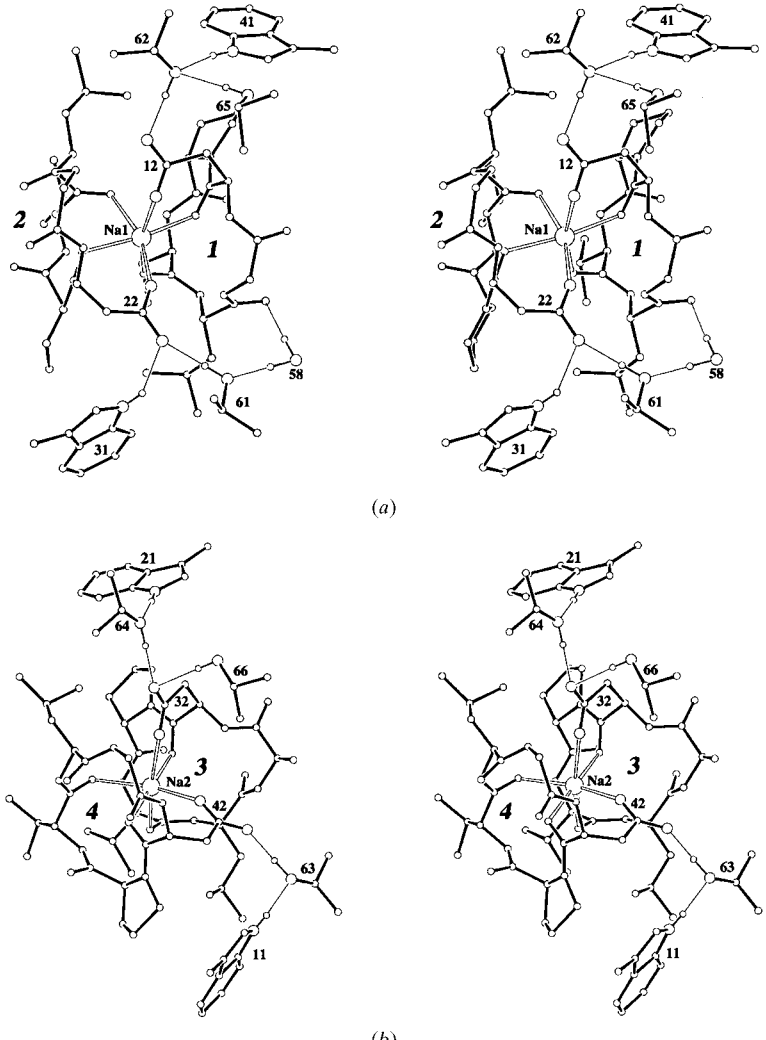

Figure 5
Stereoview of structures including iPr molecules. Figures are projected on the caged structures including (*a*) Na1 and (*b*) Na2 atoms. Obstacle side chains and H atoms are omitted to show the linkage between D-Trp, D-Asp, iPr and the sodium ion. Open bonds and thin lines represent coordination bonds and hydrogen bonds, respectively. O and N atoms related to the continuous linkages are represented by larger circles. Italic and roman numbers represent the independent molecules and residue number, respectively.

(Fig. 5*a*). In this interaction, the long-range linkage D-Trp···D-Asp—Na—D-Asp···iPr···D-Trp is observed. A similar continuous linkage is observed between the D-Trp11 and D-Trp21 residues (Fig. 5*b*). A direct hydrogen bond is not formed between D-Trp and D-Asp residues, although the hydrogen bond D-Trp···iPr···D-Asp is symmetrically formed from the Na2 atom. These relations are likely to be associated with the electron transfer between the indole ring and ion, and stabilize the coordination bonds between D-Asp and the sodium ion.

7. Discussion

The structures of the four BQ123 molecules are very similar to each other, except for the local conformations of bulky side chains which interact differently with solvent molecules. This seems to be mainly caused by the relatively tight backbone composed of five amino acids. However, it is very interesting that the low-energy models of BQ123 in CD_3OH solution (Bean *et al.*, 1994) are similar to the crystal structures in spite of sodium ion induced stress. Furthermore, the structural similarity between BQ123 and the C-terminal tail of endothelin (Peishoff *et al.*, 1995) explains the high intrinsic affinity of BQ123 and related cyclic pentapeptides of endothelin inhibitors for a sodium ion (Ngoka & Gross, 1999). The present caged and clustered structures evidently indicate the ability of BQ123 to form a complex with a sodium ion. Considering the conserved sequence of the C-termini in the endothelin families, these suggest the possibility that the C-terminal tail of endothelin has an affinity for a sodium ion. These also give a structural basis for the understanding of the protective effects of BQ123 and related cyclic pentapeptides against ischaemia-induced acute renal failure (Ngoka & Gross, 1999).

The synchrotron beam time was provided by Hyogo prefecture and Japan Synchrotron Radiation Research Institute (Approval No. C99A24XU-005N).

References

Bean, J. W., Peishoff, C. E. & Kopple, K. D. (1994). *Int. J. Pept. Protein Res.* **44**, 223–232.
Burnett, M. N. & Johnson, C. K. (1996). *ORTEP*III. Report ORNL-6895. Oak Ridge National Laboratory, Tennessee, USA.
Coles, M., Sowemimo, V., Scanlon, D., Munro, S. L. & Craik, D. J. (1993). *J. Med. Chem.* **36**, 2658–2665.
Collaborative Computational Project, Number 4 (1994). *Acta Cryst.* D**50**, 760–763.
Doi, M., Ishida, T., Katsuya, Y., Mezaki, Y., Sasaki, M., Terashima, A., Taniguchi, T., Hasegawa, H. & Shiono, M. (2000). *J. Chem. Soc. Chem. Commun.* pp. 743–744.

Fukami, T., Nagase, T., Fujita, K., Hayama, T., Niiyama, K., Mase, T., Nakajima, S., Fukuroda, T., Saeki, T., Nishikibe, M., Ihara, M., Yano, M. & Ishikawa, K. (1995). *J. Med. Chem.* **38**, 4309–4324.
Guex, N. & Peitsch, M. C. (1997). *Electrophoresis*, **18**, 2714–2723.
Gulati, A. (1995). *Endothelin: Role in Health and Disease.* London: Harwood Academic Publishers.
Hewage, C. M., Jiang, L., Parkinson, J. A., Ramage, R. & Sadler, I. H. (1997). *J. Pept. Sci.* **3**, 415–428.
Ihara, M., Fukuroda, T., Saeki, T., Nishikibe, M., Kojiri, K., Suda, H. & Yano, M. (1991). *Biochem. Biophys. Res. Commun.* **178**, 132–137.
Ihara, M., Noguchi, K., Saeki, T., Fukuroda, T., Tsuchida, S., Kimura, S., Fukami, T., Ishikawa, K., Nishikibe, M. & Yano, M. (1992). *Life Sci.* **50**, 247–255.
Ishikawa, K., Fukami, T., Nagase, T., Fujita, K., Hayama, T., Niiyama, K., Mase, T., Ihara, M. & Yano, M. (1992). *J. Med. Chem.* **35**, 2139–2142.
Janes, R. W., Peapus, D. H. & Wallace, B. A. (1994). *Nature Struct. Biol.* **1**, 311–319.
Kojiri, K., Ihara, M., Nakajima, S., Kawamura, K., Funaishi, K., Yano, M. & Suda, H. (1991). *J. Antibiot.* **44**, 1342–1347.
Leslie, A. G. W. (1990). *Crystallographic Computing.* Oxford University Press.
Matsugaki, N. & Shiono, M. (1998). *LODEM. A Density Modification Program for Ab Initio Solution of Crystal Structures from X-ray Diffraction Data.* Kyushu University, Kyushu, Japan.
Matsui, J., Kagoshima, Y., Tsusaka, Y., Katsuya, Y., Motoyama, M., Watanabe, Y., Yokoyama, K., Takai, K., Takeda, S. & Chikawa, J. (1997). *SPring-8 Annual Report 1997*, edited by Y. Miyahara, pp. 125–130. Hyogo: Japan Synchrotron Radiation Research Institute.
Nakajima, S., Niiyama, K., Ihara, M., Kojiri, K. & Suda, H. (1991). *J. Antibiot.* **44**, 1348–1356.
Ngoka, L. C. & Gross, M. L. (1999). *Biochem. Biophys. Res. Commun.* **257**, 13–19.
Okada, K., Takeda, J., Arai, Y., Matsuyama, K. & Yano, M. (1991). *Biochem. Biophys. Res. Commun* **180**, 1019–1023.
Peapus, D. H., Janes, R. W. & Wallace, B. A. (1993). *J. Mol. Biol.* **234**, 1250–1252.
Peishoff, C. E., Janes, R. W. & Wallace, B. A. (1995). *FEBS Lett.* **374**, 379–385.
Sheldrick, G. M. (1997). *SHELXS*97. *Program for the Solution of Crystal Structures from Diffraction Data.* University of Göttingen, Göttingen, Germany.
Van der Walle, C. F., Bansal, S. & Barlow, D. J. (1998). *J. Pharm. Pharmacol.* **50**, 837–44.
Verbist, J., Putzeys, J.-P., Piret, P. & van Meerssche, M. (1971). *Acta Cryst.* B**27**, 1190–1195.
Yanagisawa, M., Kurihara, H., Kimura, S., Tombe, Y., Kobayashi, M., Mitsui, Y., Yazaki, Y., Goto, K. & Masaki, T. (1988). *Nature (London)*, **332**, 411–415.